Energy, Mines and Resources Canada | Énergie, Mines et Ressources Canada

CANMET

Canada Centre for Mineral and Energy Technology | Centre canadien de la technologie des minéraux et de l'énergie

HYDROCRACKING BOSCAN HEAVY OIL WITH A Co-Mo-A_2O_3 CATALYST CONTAINING AN H-MORDENITE ZEOLITE COMPONENT

R.J.A. Minja and M. Ternan
Synthetic Fuels Research Laboratory

APRIL 1990

ENERGY RESEARCH LABORATORIES
DIVISION REPORT 90-31 (J)

This work was supported in part by the Federal Panel on Energy Research and Development (PERD)

HYDROCRACKING BOSCAN HEAVY OIL WITH A Co-Mo/Al_2O_3 CATALYST CONTAINING AN H-MORDENITE ZEOLITE COMPONENT

by

Rwaichi J.A. Minja[1]
Department of Chemical Engineering
University of Ottawa
Ottawa, Ontario, K1N 9B4, Canada

and

Marten Ternan*
Energy Research Laboratories / CANMET
Energy, Mines and Resources, Canada
Ottawa, Ontario, K1A 0G1, Canada

Co-Mo/Al_2O_3 catalysts for hydrocracking heavy oil and residua were modified by adding up to 20 wt % hydrogen mordenite zeolite. The acidic sites on the external surface of the mordenite crystals were expected to increase cracking reactions. In fact, there was a slight decrease in the +525°C resid conversion, although vanadium and nickel hydrodemetallization increased as the mordenite content of the catalyst increased. On the other hand, the pseudo turnover frequency for metals removal, i.e., the number of reactions per second per reaction site (or in this case per $(nm)^2$), was greater for catalysts containing greater amounts of mordenite. The catalyst performance was attributed to a combination of two factors. First, both the catalyst bulk density (grams of catalyst per milliliter of reactor volume) and the catalyst specific surface area (m^2/g) in pores larger than 3 nm, decreased as the mordenite content increased. Hence, a smaller quantity of catalyst could be placed into the reactor and the catalyst that was in the reactor had less surface area per unit mass. Clearly the mordenite changed the structure of the alumina support, which resulted in a net decrease in the effective catalyst surface area. Second, the catalyst acidity, as measured by temperature programmed desorption of benzofuran, increased as the mordenite component of the catalyst increased. It was concluded that the improved overall hydrodemetallization was caused by both the increased number of acidic sites on the exterior surfaces of the mordenite and the changes in catalyst pore geometry, which improved the rate of diffusion to the catalyst surface.

1. Permanent Address: Department of Chemical and Process Engineering, University of Dar Es Salaam, Box 35131, Dar es Salaam, Tanzania

* to whom correspondence should be addressed

HYDROCRACKING BOSCAN HEAVY OIL WITH A Co-Mo/Al_2O_3 CATALYST CONTAINING AN H-MORDENITE ZEOLITE COMPONENT

by

Rwaichi J.A. Minja
Department of Chemical Engineering
University of Ottawa
Ottawa, Ontario, K1N 9B4, Canada

and

Marten Ternan
Energy Research Laboratories / CANMET
Energy, Mines and Resources, Canada
Ottawa, Ontario, K1A 0G1, Canada

INTRODUCTION

The primary objective of hydrocracking is to decrease the size of the large molecules in the +525^{o}C fraction of heavy oils, bitumens, and petroleum vacuum residua. The removal of heteroatoms, sulphur, nitrogen, oxygen, and metals is also of considerable importance. The remaining unconverted +525^{o}C residuum, after hydrocracking, is frequently used as a feedstock for coking processes. Often the concentrations of sulphur and nitrogen in the coke prohibit its use for combustion. In many cases, the metals concentration in the coke is also too large, so it cannot be used for electrode coke. The Boscan heavy oil used in this work has one of the highest metal concentrations in residual oils (1). Therefore hydrodemetallatization (HDM) was of particular interest.

Catalytic cleavage of the chemical bonds between atoms is normally related to the acidic properties of a catalyst. Both the conversion of large molecules into small molecules and metals removal require bond breaking. In this work, a hydrogen mordenite zeolite was added, as an additional component, to a conventional Co-Mo-Al_2O_3 hydrocracking catalyst. Mordenite is one of the most acidic zeolites (2). The effect of the mordenite addition on the catalyst and on the conversion of the heavy oil are discussed in the work reported here.

EXPERIMENTAL SECTION

Six different Co-Mo-Al_2O_3 catalysts were prepared, having the hydrogen mordenite contents shown in Table 1. The H-mordenite was purchased from Union Carbide (product number LZM8). Alpha alumina monohydrate (Catapal SB from Continental Oil Company) powder was mixed with appropriate amounts of ammonium paramolybdate (dissolved in aqueous ammonium hydroxide) solution, cobalt nitrate solution, distilled water, and nitric acid to form a paste. The catalyst without the H-mordenite zeolite was made directly from this paste.

For each of the H-mordenite containing catalysts, an oil - mordenite paste was mixed with the above alumina paste. The H-mordenite crystals were placed in a beaker and mixed while a light distillate oil was added drop wise to form a homogeneous oil paste. Approximately 1.4 mL of oil was used per gram of H-mordenite. It was expected that surrounding the mordenite with oil would prevent the alumina paste from either entering the mordenite pore structure or from blocking the exterior surfaces of the mordenite from contact with the feedstock.

The final catalysts were obtained by mixing appropriate amounts of the two pastes and extruding with a hand extruder. The extrudates were dried at 110°C for approximately 10 hours, and calcined in air at 450°C for 4.5 hours. This procedure would remove the moisture and burn off the light oil. The catalyst geometry was measured by mercury porosimetry (pore size distribution) and nitrogen adsorption (surface area). All catalysts contained close to 15 wt % MoO_3 and 3 wt % CoO, as shown in Table 1.

High pressure hydrocracking experiments with Boscan heavy oil were used to

evaluate the catalysts. Properties of the feedstock are shown in Table 2. The feedstock mixed with hydrogen flowed through a preheater which raised the temperature to 300°C and then flowed into the bottom of the reactor which contained a fixed bed of one of the catalysts. The reactor had an internal volume of 155 mL and a length to diameter ratio of 12. After presulphiding at 400°C with the heavy oil, hydrocracking experiments were performed at a pressure of 13.9 MPa, a temperature of 400°C, a liquid space velocity (LSV) of 1.0 h^{-1} based on the empty reactor volume, and a hydrogen flow rate of 36 mL s^{-1} (5000 scf/bbl). A description of the equipment has been given elsewhere (3).

The liquid products were analyzed for microcarbon residue (MCR) content, a measure of coke precursors, using an Alcor MCRT analyzer (4). Vanadium and nickel analyses were performed by dissolving samples of the hydrocarbon product in xylene and making atomic adsorption measurements.

RESULTS AND DISCUSSION

Figure 1 shows the calculated conversion of the +525°C residuum. It was calculated from a correlation (5) between weight per cent +525°C residuum and weight per cent MCR. Apparently, the addition of mordenite to the catalyst did not influence the overall conversion of residuum. This observation will be discussed further after the geometrical properties of the catalysts have been considered.

Figure 2 shows the weight per cent vanadium conversion and the weight per cent nickel conversion as a function of the amount of mordenite in the catalyst. It is readily apparent that the addition of the mordenite component to the catalyst increases the conversion of the organo-metallic vanadium and nickel complexes that are in the heavy oil. These residuum molecules are too large to enter the small pores of the mordenite. One possible explanation is that the acid sites (6) on the external surfaces of the zeolite crystals were responsible for the increased conversion. Catalytic cracking of gas oils, which are composed of smaller molecules, has also been attributed to the external sites on zeolite crystals (7).

The above hydrodemetallization (HDM) results can be considered in terms of the geometrical properties of the catalysts, which produced them. The geometrical

properties are shown in Table 3. The amount of catalyst that could be loaded into the reactor decreased as the catalyst mordenite content increased. Part of this was caused by the decrease of the catalyst extrudate particle density with increasing mordenite content of the catalyst. However, this was not the only factor. As the catalyst mordenite content increased, the extrudate shapes became more and more curved. This caused the extrudate shapes to pack more loosely in the reactor with more space between them. Therefore the catalyst bulk density decreased with increasing mordenite.

Table 3 shows that the catalyst surface area was measured in two different ways. The surface area measured by nitrogen adsorption, following the method of Brunauer, Emmett and Teller (BET) increased as the catalyst mordenite content increased. This would be expected, since the micropores formed by the cages within the mordenite crystal structure have large surface areas. In contrast the surface area measured by mercury porosimetry decreases as the catalyst mordenite content increases. This is because the mercury is only forced into pores having a diameter, D_p, larger than 3 nm. Since the mercury does not enter the mordenite micropores, mercury porosimetry only measures the surface area of the alumina. As the catalyst mordenite content increases, the alumina content decreases. This explains the decrease in mercury porosimetry surface area with increasing catalyst mordenite content. The heavy oil molecules have diameters close to 4 nm (8) and therefore will not be able to enter the mordenite. The sodium form of mordenite has pore diameters of 0.67 - 0.7 nm (9) and the diameters in the hydrogen form are only slightly larger (10). The mercury porosimetry surface areas were used in this work, because they are more likely to represent the surface area available to the resid molecules.

The total surface area in the reactor can be obtained by multiplying the surface area per gram by the weight of catalyst loaded into the reactor. These quantities, listed in Table 3, indicate that there was a substantial decrease in surface area as larger amounts of mordenite were added to the catalyst. The HDM conversions in Figure 2 can be divided by the surface area in the reactor and the units changed to obtain a pseudo turn over frequency (PTOF), for example atoms vanadium removed per second per square nanometer. In this way the results are expressed per unit of available surface area. If the number of reaction sites per square nanometer were known, then the real turn over frequency (TOF) could have been

used as the reaction coordinate.

Because the bulk density of the catalyst changed as the mordenite content increased, the void volume in the reactor also changed. The volume of catalyst can be calculated by dividing the weight of catalyst in the reactor by the catalyst extrudate particle density. The void volume is obtained by subtracting the catalyst volume from the volume of the empty reactor. The residence time of the resid molecules in the reactor increases with increasing void volume. To account for this the reaction coordinate can be expressed in terms of PTOF per second of residence time (PTOF/Θ) in the reactor.

Figure 3 shows that the PTOF/Θ for vanadium and nickel HDM increases linearly as mordenite is added to the catalyst. As mentioned above, this might be explained by the increasing number of acid sites on the external surfaces of the mordenite crystals. However, it is also important to consider possible changes in diffusion within the catalyst, that could result from the changes in catalyst internal geometry.

A similar graph of PTOF/Θ could be shown for the +525^{o}C resid. It would also indicate a linear increase with increasing mordenite content of the catalyst. This phenomenon is one of the effects that produce the horizontal line in Figure 1. A compensating effect was the decrease in catalyst surface area inside the reactor as mordenite is added to the catalyst. When all the factors are combined the net effect was that the overall conversion in Figure 1 did not change significantly when mordenite was added to the catalysts.

The mercury porosimetry results in Figure 4 show the volume of mercury that penetrated the catalyst containing 10 % mordenite, as the pressure on the mercury surrounding the catalyst increased. The equation of Young and LaPlace was used to calculate the pore diameter, D_p, from the pressure at which the mercury penetrated the catalyst. For this catalyst, most of the pores are in two size ranges, 1-10 μm and 5-10 nm. All of the catalysts contained pores in exactly the same size ranges. The only difference was that the pore volume in each size range changed as mordenite was added to the catalyst.

Figure 5 shows the volume of catalyst pores within three different size

ranges, as a function of the amount of mordenite in the catalyst. The three ranges are 3 nm < D_p < 10 nm; 10 nm < D_p < 10 μm; and 10 μm < D_p. The greatest difference is between the catalyst without mordenite and the one with 1 % mordenite. The pore volume change for D_p > 10 um was very small. The largest pore volume change was for the macropores in the range 10 nm < D_p < 10 μm.

The results in Figure 5 suggest that the colloidal particle structure of the alumina has been disrupted by the addition of mordenite crystals. One can speculate that the pore volume changes may have occurred when the catalyst was dried and calcined. When the catalyst was in the paste form, an oil layer surrounded the mordenite crystals and separated them from the aqueous alumina. When drying occurred it is possible that spaces between the alumina and the mordenite developed. Figure 5 shows that most of the additional pore volume (or perhaps most of these spaces) are in the size range 10 μm > D_p > 10 nm, with a smaller volume in the 3 nm < D_p < 10 nm range. These spaces would not be present in the pure alumina catalyst, since no mordenite and therefore no oil layer was present.

The upper part of Figure 6 illustrates the spaces between the alumina and the mordenite. It is also shown in a highly idealized way in the lower part of Figure 6. For a given value of pore volume, considerable surface area is created when the pore volume is in pores of small D_p, and relatively little surface area is created when the pore volume is in pores of large D_p. Since most of the additional pore volume created is in the 10 μm > D_p > 10 nm pore range, the lower part of Figure 6 has been drawn to show the additional pore volume in larger pores which provide additional access to the surface area in the small pores.

The pore volume per unit surface area is shown in Table 3. One interpretation is that the pore volume available for access to the catalyst surface area has increased as mordenite was added to the catalyst. This suggests that the rate of diffusion to the catalyst surface would increase. In Figure 7 the PTOF/Θ is correlated with the catalyst pore volume per unit surface area (V_p/A_s). In this graph both the ordinate and the abscissa are expressed on a unit surface area basis.

If the reaction rate, R, was controlled by diffusion, then

$$R = N A_x \qquad (1)$$

where N is the flux (mols per unit time per unit cross sectional area) and A_x is the cross sectional area. According to Equation 1, the reaction rate, R, should increase by the same factor as the cross sectional area, A_x. For these catalysts the pore diameters are similar in all catalysts, so N will not change because D_p has affected the effective diffusivity, D_{eff}. What changes is the ratio of pore volume per unit surface area, V_p/A_s. The maximum increase in A_x would occur if A_x was proportional to the increase in V_p/A_s.

Figure 7 shows PTOF/Θ plotted versus V_pA_s. It is apparent that the slope of the curve is much smaller when the H-mordenite content of the catalyst increases from 0 % to 1 % (V_p/A_s increases from 1.7 to 2.26 x 10^{-3}), than when it increases from 1 % to 20 %. It should be noted, in Figure 5 that most of the increase in pore volume occurred as the H-mordenite content of the catalyst increased from 0 to 1 %. From Equation 1, it can be seen that an increase of the cross sectional area by some factor should cause an increase the reaction rate by the same factor. Therefore, ignoring powers of ten, any slope of 1 or less would indicate that diffusion could be responsible for the increase in PTOF/Θ. The slopes in Figure 7 from H-mordenite contents of 0 to 1 % are 0.63 x 10^{-5} and 0.36 x 10^{-6} for vanadium and nickel respectively. This indicates that diffusion could account for the increased PTOF/Θ between 0 an 1 % H-mordenite content.

The slopes of straight lines between the points in Figure 7 for the catalysts containing 1 % and 20 % H-mordenite are much steeper. These slopes are 5.1 x 10^{-5} and 3.1 x10^{-6} for vanadium and nickel respectively. Since these factors are much greater than 1, it is clear that diffusion can not be the only explanation for the increase in PTOF/Θ as the catalyst H-mordenite content is increased from 1 % to 20 %. Instead the increase in PTOF/Θ is also attributed to the acid sites on the exterior of the additional H-mordenite crystals that are in the catalysts.

The catalyst surface acidity was measured by adsorbing benzofuran on the catalysts and then performing temperature programmed desorption (TPD). Some TPD results are shown in Figure 8. The peak at 120°C increased (and became a shoulder

in the catalyst containing 20 % H-mordenite) when more mordenite was present in the catalyst. The increase in the high temperature peaks (120 and 130^{o}C) is taken as an increase in the number of acidic sites. Thus the improved HDM conversions caused by the mordenite component can be attributed partly to improved diffusion toward the catalyst surface and partly to the increased number of acid sites on the external surfaces of the mordenite crystals.

CONCLUSIONS

The addition of hydrogen mordenite to a Co-Mo-Al_2O_3 catalyst affected several geometric properties of the catalyst. The catalyst bulk density, extrudate particle density, and surface area measured by mercury porosimetry all decreased. However the catalyst pore volume per unit surface area increased, suggesting an enhancement in the rate of diffusion of the large resid molecules toward the reaction sites on the catalyst surface area.

The addition of hydrogen mordenite caused an enhancement in HDM when measured either in terms of overall conversion or in terms of PTOF. This enhancement was attributed to two factors. A greater rate of diffusion to the reaction sites was caused by the increased catalyst pore volume. A greater rate of reaction on the catalyst surface was attributed to the increase in number of reaction sites, caused by the acidity of additional mordenite crystals' external surfaces.

REFERENCES

1. Quann, R.J.;Ware, R.A.;Hung, C.W.;Wei, J.; Adv. Chem. Eng., 1988, 14, p.100.

2. Dwyer, A.; An Introduction to Zeolite Molecular Sieves; Wiley; New York, 1988; p.123.

3. Kelly,J.F.;Ternan,M.; Can. J. Chem. Eng. 1979, 57, 726-733.

4. ASTM Method D-4530, Annual Book of ASTM Standards - Petroleum Products, Lubricants, and Fossil Fuels 5.02 ASTM; Philadelphia, 1987; pp.585-590.

5. Ternan, M.;Kriz, J.F.;AOSTRA J. Res. 1990 (accepted for publication)

6. Decroocq, D.: Catalytic Cracking of Heavy Petroleum Fractions; Gulf and Technip; Houston and Paris, 1984; pp.16-23.

7. Wojciechowski, B.W.;Corma, A.; Catalytic Cracking Marcel Dekker; New York, 1986; pp. 80-82.

8. Kryriacou, K.C.;Baltus, R.E.;Rahimi, P.; Fuel 1988 67, 109-113.

9. Bolton, A.P.; Molecular Sieve Zeolites in Experimental Methods in Catalytic Research 2 (ed. R.B. Anderson); Academic Press; New York, 1976; pp.21-23.

10. Ruthven, D.M.; Principles of Adsorption and Adsorption Processes Wiley, New York; 1984; p.16.

TABLE 1

CATALYST CHEMICAL COMPOSITION

H-Mordenite wt %	Al_2O_3 wt %	SiO_2 wt %	MoO_3 wt %	CoO wt %
0	81.5	0.0	15.4	3.1
1	81.2	0.3	15.3	3.1
3	80.0	1.7	15.1	3.1
5	78.9	3.2	14.9	3.1
10	76.5	6.0	14.4	3.0
20	72.4	11.2	13.5	2.9

TABLE 2

PROPERTIES OF BOSCAN HEAVY OIL

Specific Gravity (15°C)	1.004
Carbon (wt %)	81.8
Hydrogen (wt%)	10.4
Nitrogen (wt%)	0.64
Sulphur (wt %)	5.38
Vanadium (ppm)	1385
Nickel (ppm)	107
Pentane Insolubles (wt %)	20.1
Toluene Insolubles (wt %)	0.1
Ash (wt %)	0.22
+525°C Residue (wt %)	54.6

TABLE 3

CATALYST PHYSICAL CHARACTERISTICS

Zeolite in Catalyst wt %	Catalyst in Reactor g	BET Surface Area m^2/g	Hg Poros Surface Area m^2/g	Catalyst Particle Density g/mL	Catalyst Pore Volume mL/g	Pore Volume per unit Surface Area $mL/^2$
0	93.9	193	194	1.44	0.33	1.70
1	86.7	205	195	1.27	0.44	2.26
3	75.8	202	191	1.22	0.45	2.36
5	67.8	203	196	1.21	0.47	2.40
10	76.8	208	184	1.23	0.45	2.45
20	57.0	215	169	1.191	0.42	2.49

CAPTIONS FOR FIGURES

Figure 1 - +525^{o}C Resid Conversion (wt %) Calculated from MCR Measurements Versus wt % H-Mordenite in Catalyst.

Figure 2 - Metal Conversion (wt %) Versus wt % H-Mordenite in Catalyst. Open and solid circles represent vanadium and nickel respectively.

Figure 3 - Pseudo Turnover Frequency per Unit Residence Time (atoms metal removed per $(nm)^2$ per s^2) Versus wt % H-Mordenite in Catalyst. The numbers on the ordinate have been multiplied by 10^8 and 10^9 for vanadium and nickel respectively. Open and solid circles represent vanadium and nickel respectively.

Figure 4 - Volume of Mercury in Catalyst Pores (mL/g) Versus the Pressure Applied to the Mercury (MPa) for a Catalyst Containing 10 wt % H-Mordenite. The lower curve represents mercury penetration into the catalyst pores and the upper curve represents mercury retraction from the catalyst pores.

Figure 5 - Volume of Mercury in Catalyst Pores of a Particular Size Range (mL/g) Versus wt % H-Mordenite in the Catalyst. Open triangles represent pores having diameters between 3 and 10 nm. Solid circles represent pores having diameters between 10 nm and 10 um. Open circles represent pores having diameters greater than 10 um.

Figure 6 - Upper: Schematic Diagram of Colloidal Alumina Particles in the Catalyst. A - Alumina Particles only. B - Mordenite Crystal Surrounded by Alumina Particles. Lower: (B) shows Greater Pore Volume giving more access to the Catalyst Surface than (A).

Figure 7 - Pseudo Turnover Frequency per Unit Residence Time (atoms metal removed per $(nm)^2$ per s^2) Versus Pore Volume in Catalyst per Unit Catalyst Surface Area (mL/m^2) x 10^{-3}. The numbers on the ordinate have been multiplied by 10^{8} and 10^{-9} for vanadium and nickel respectively. Open and solid circles represent vanadium and nickel respectively.

Figure 8 - Benzofuran Temperature Programmed Desorption. Change in Weight per Unit Time (% of sample per minute) Versus Temperature (^{o}C). The Curves are labelled by H-mordenite content, 0 %, 10 % and 20 % respectively. Peaks at 90, 120, and 130^{o}C are indicated.

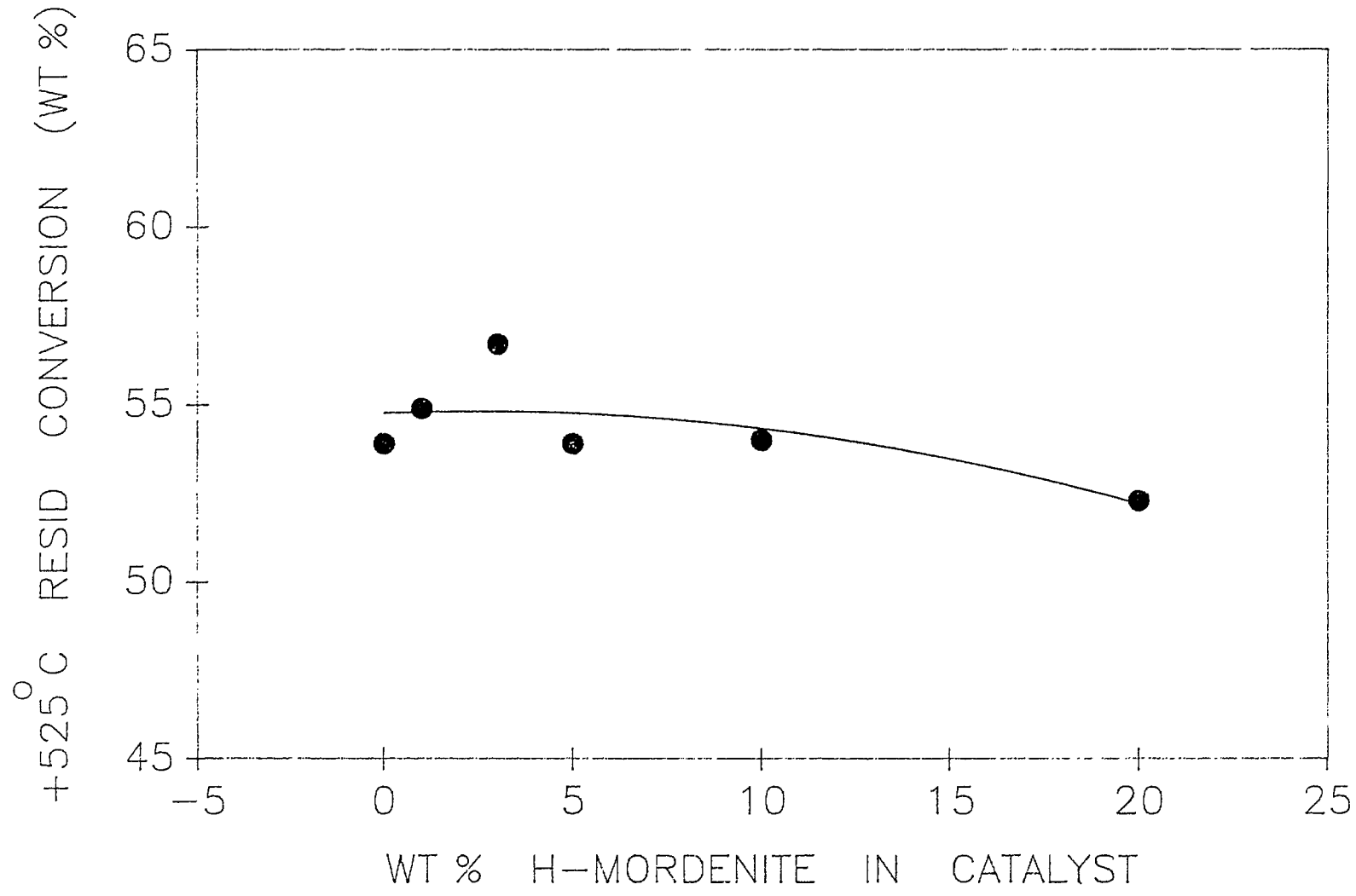
+525°C RESID CONVERSION (WT %)
65
60
55
50
45
−5
0
5
10
15
20
25
WT % H−MORDENITE IN CATALYST

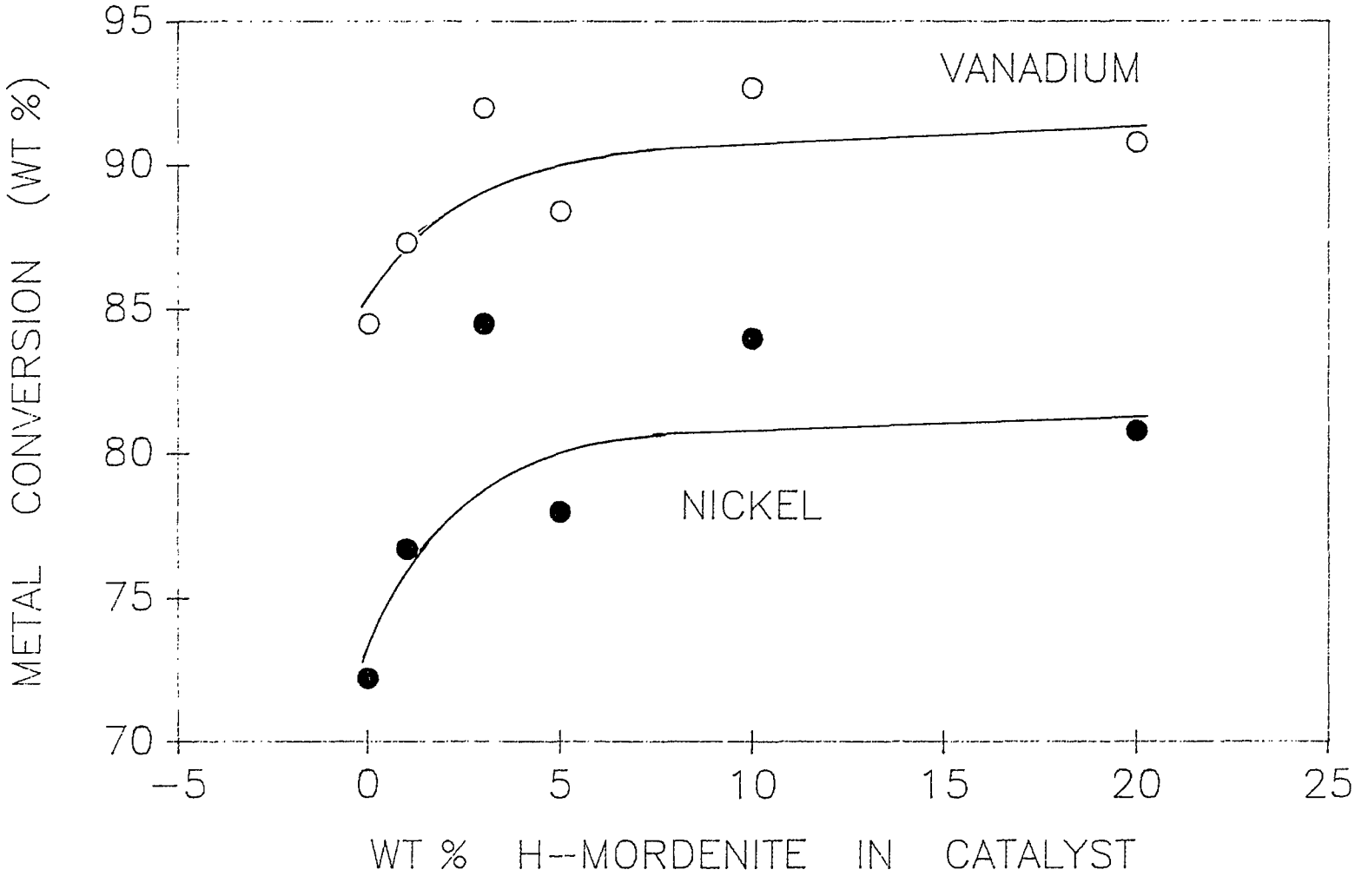
95
90
85
80
75
70
METAL CONVERSION (WT %)
VANADIUM
NICKEL
−5
0
5
10
15
20
25
WT % H--MORDENITE IN CATALYST

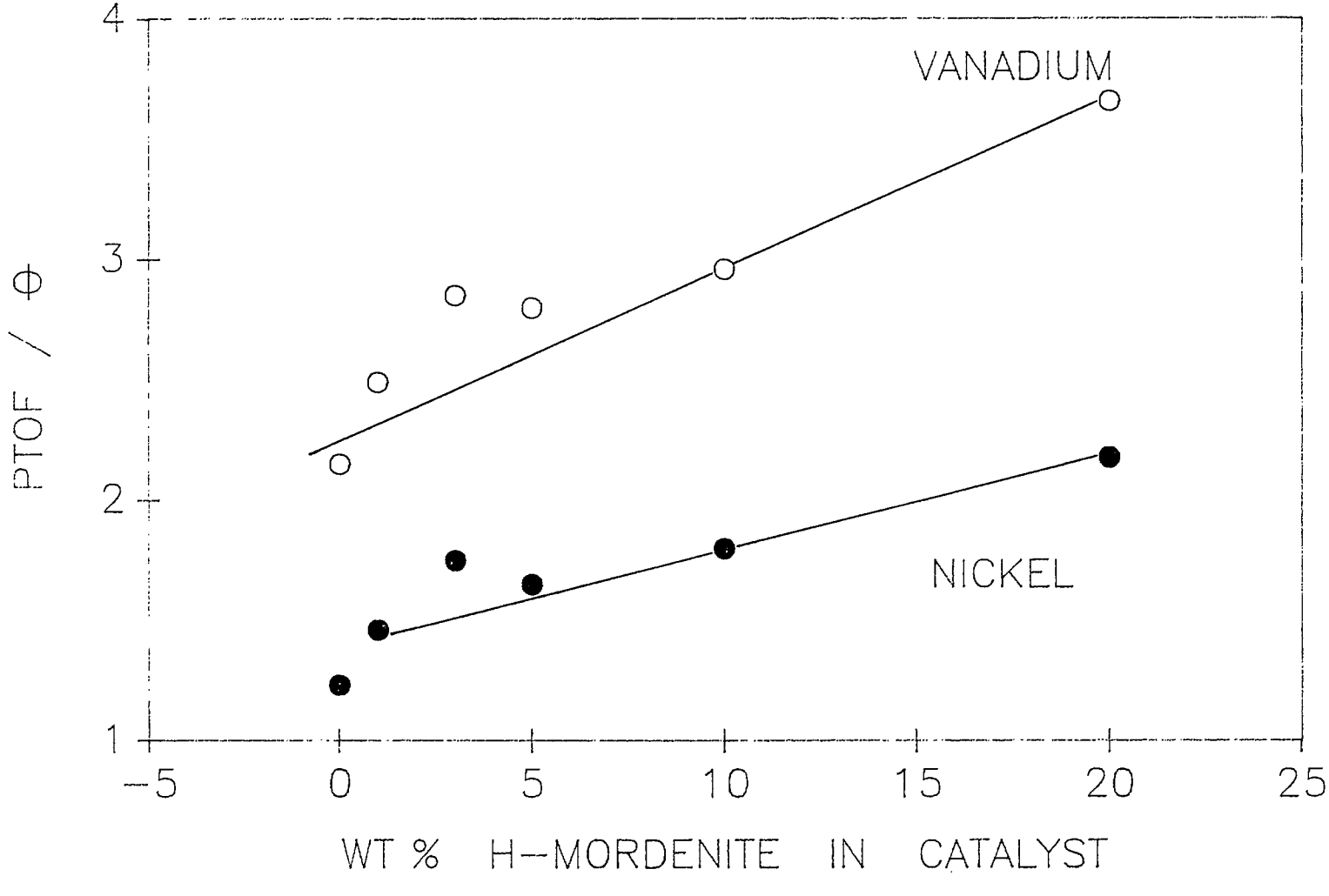
VANADIUM
NICKEL
PTOF / Φ
WT % H-MORDENITE IN CATALYST
4
3
2
1
-5
0
5
10
15
20
25

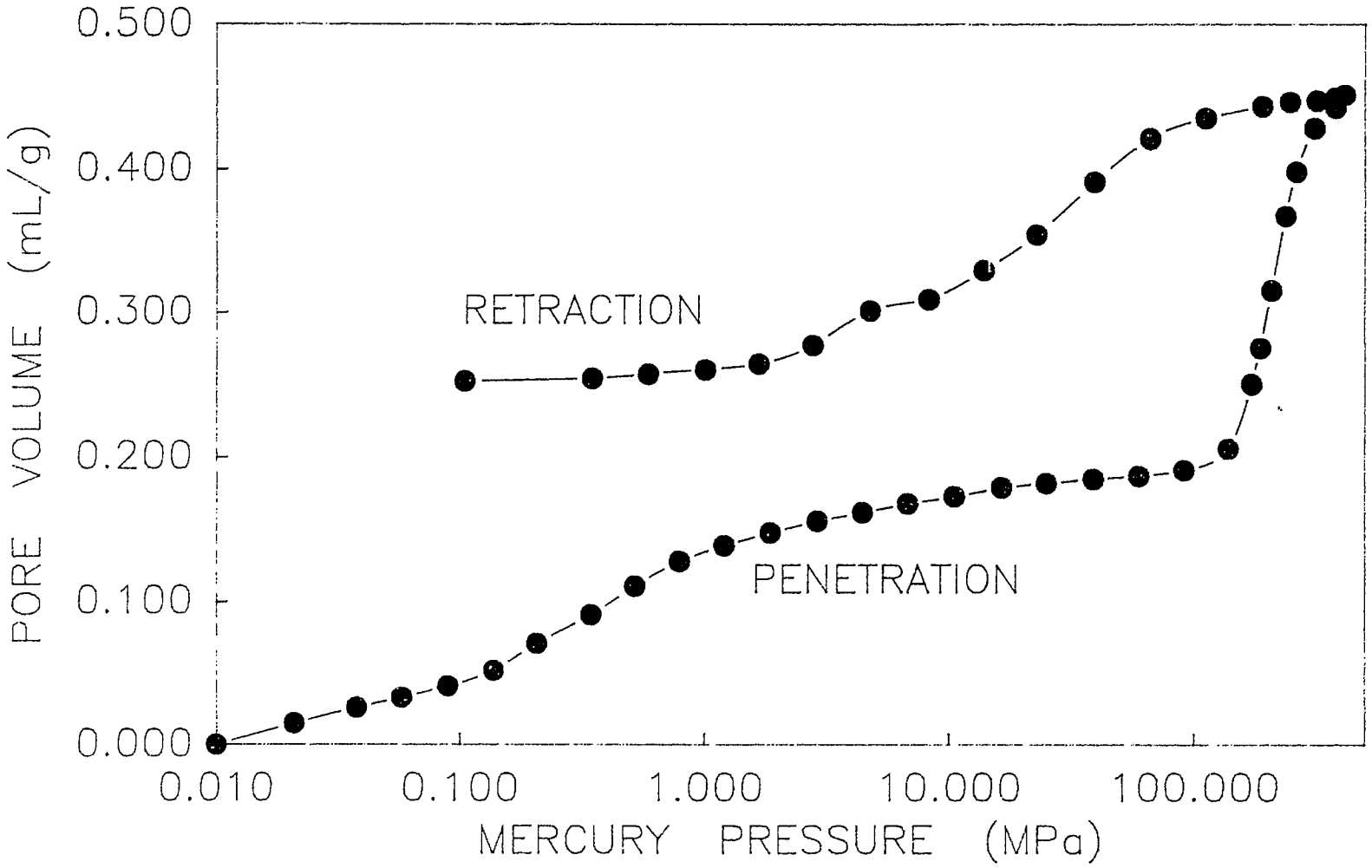
0.500
0.400
0.300
0.200
0.100
0.000
PORE VOLUME (mL/g)
RETRACTION
PENETRATION
0.010
0.100
1.000
10.000
100.000
MERCURY PRESSURE (MPa)

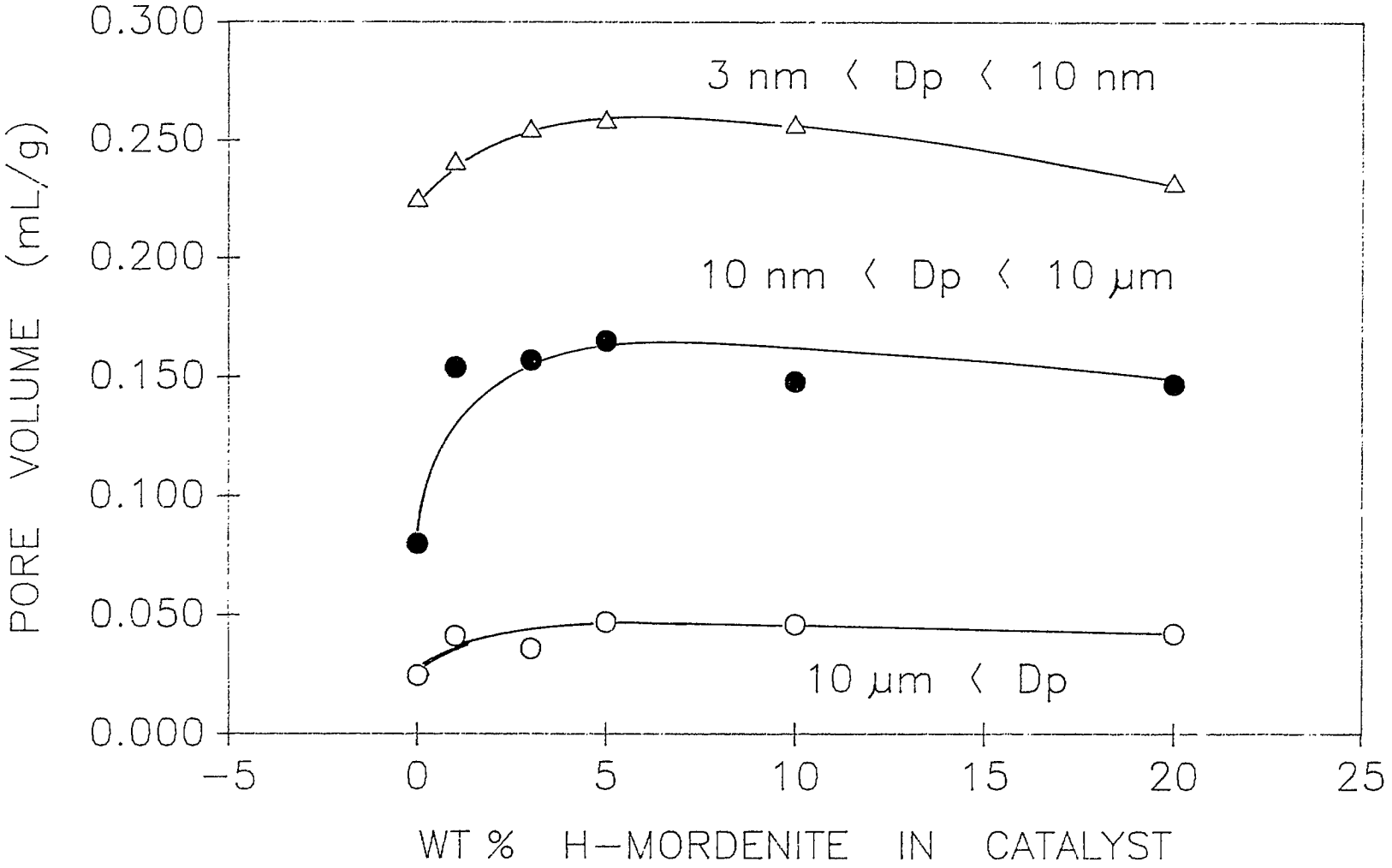
0.300
0.250
0.200
0.150
0.100
0.050
0.000
PORE VOLUME (mL/g)
3 nm < Dp < 10 nm
10 nm < Dp < 10 µm
10 µm < Dp
−5
0
5
10
15
20
25
WT % H−MORDENITE IN CATALYST

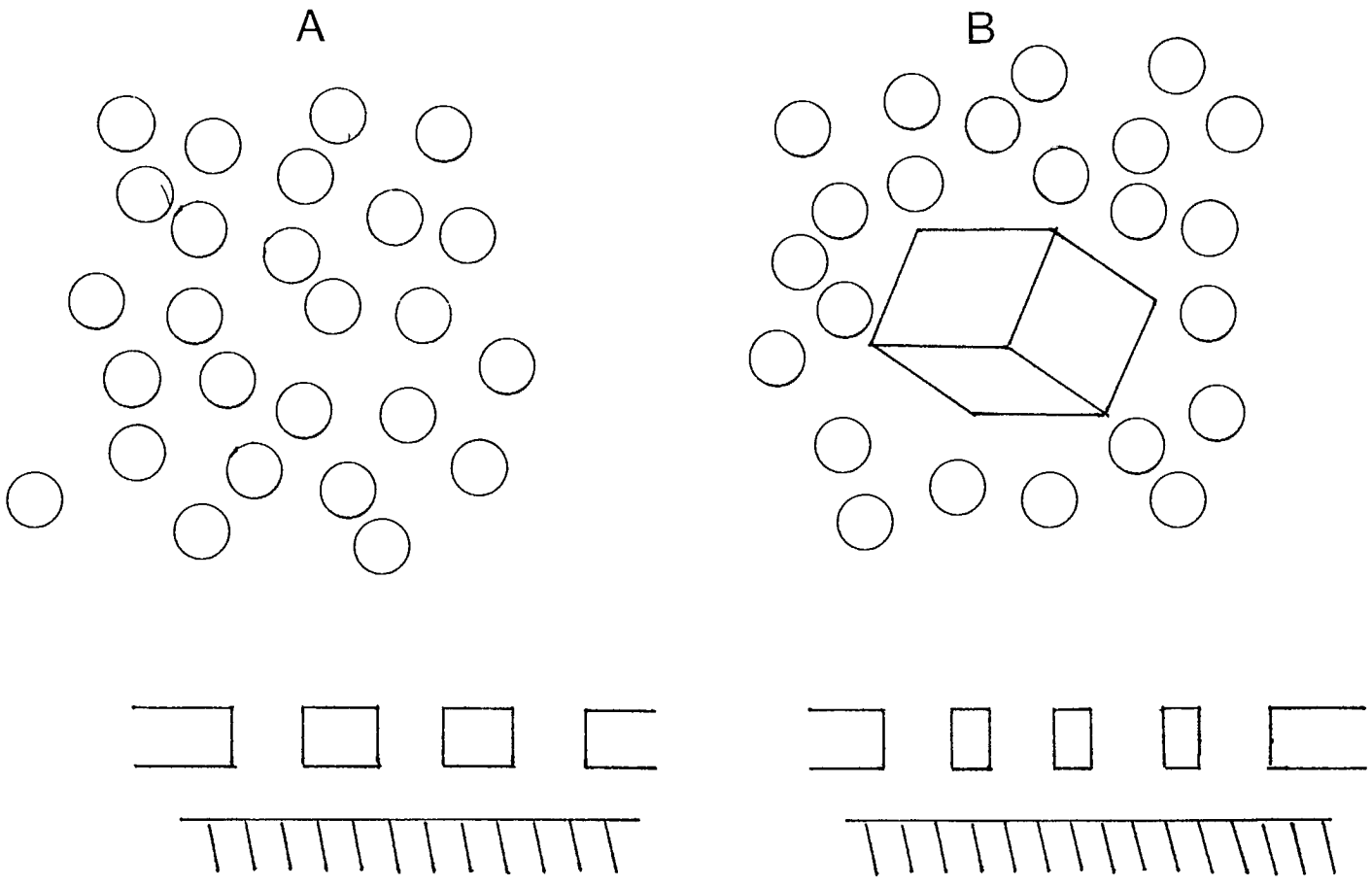
A
B

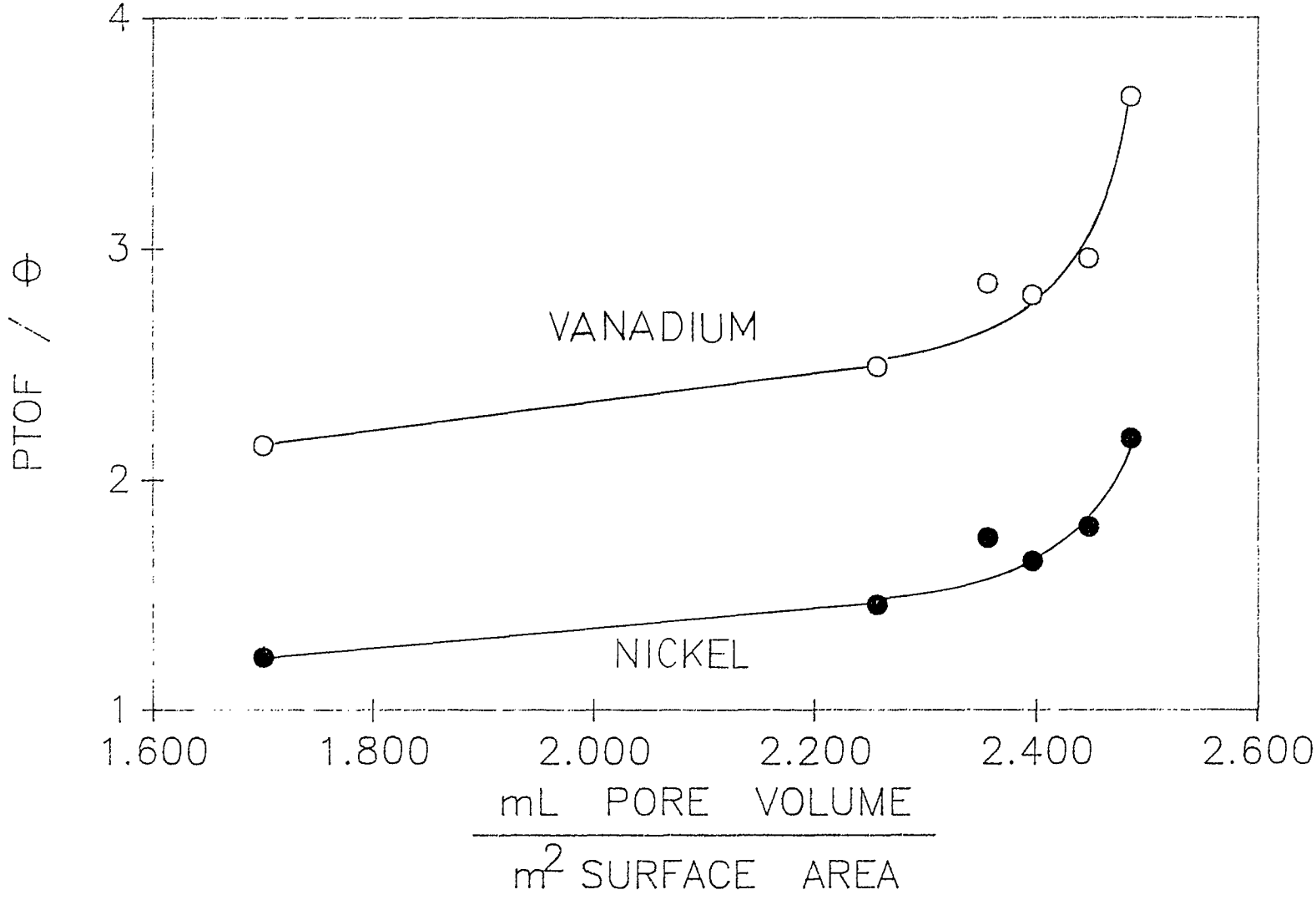
4
3
2
1
PTOF / Φ
VANADIUM
NICKEL
1.600
1.800
2.000
2.200
2.400
2.600
mL PORE VOLUME
m² SURFACE AREA

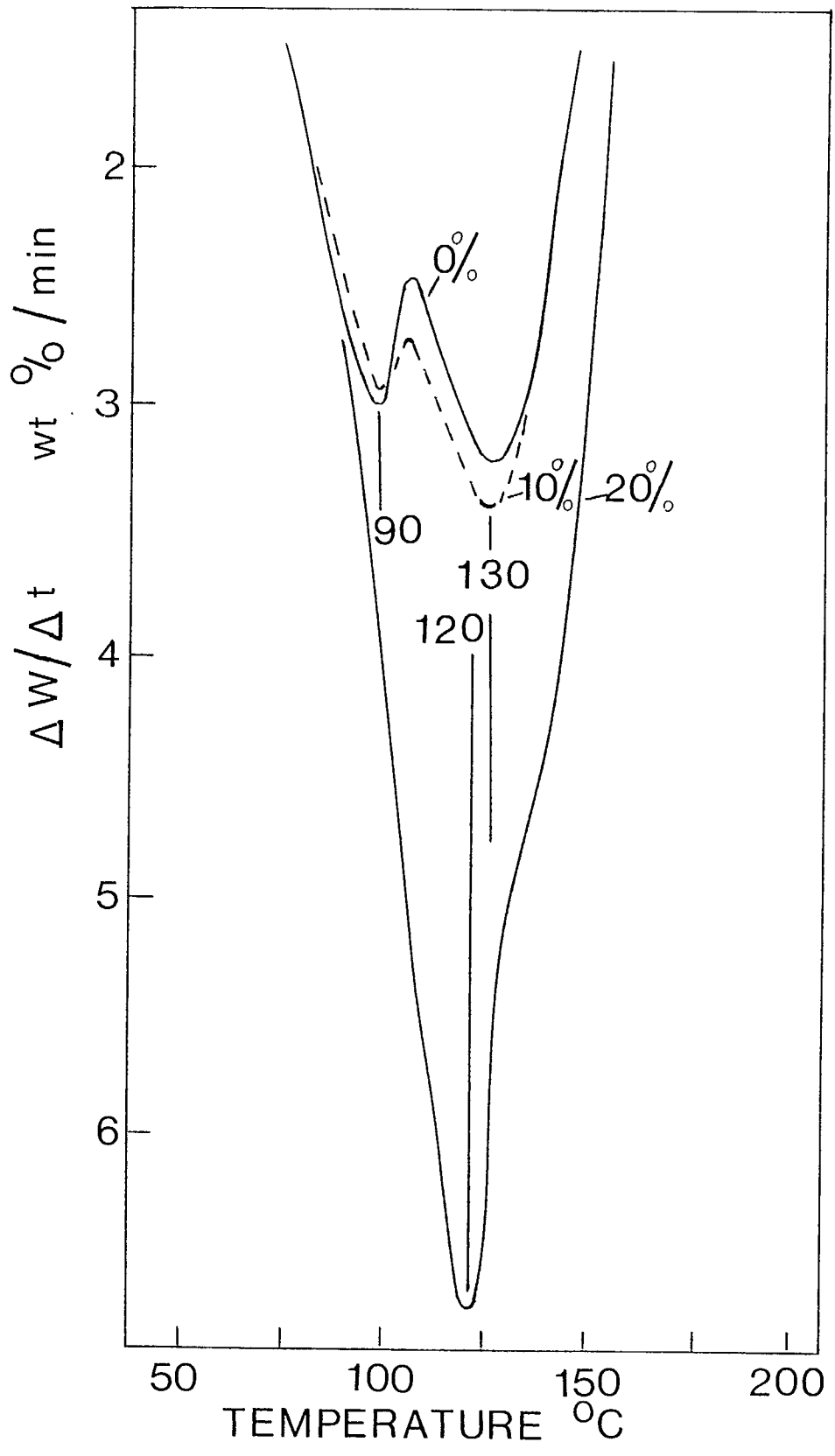
2
3
4
5
6
ΔW/Δt wt %/min
0%
10%
20%
90
130
120
50
100
150
200
TEMPERATURE °C